REMOVAL OF MANGANESE IN CONTAMINATED GROUNDWATER BY PERMEABLE REACTIVE BARRIERS USING COMPOST AND ZERO VALENT IRON

Wahyu Wilopo[1], Doni Prakasa Eka Putra[1], and Tsuyoshi Hirajima[2]

[1] Geological Engineering, Gadjah Mada University, Yogyakarta, Indonesia,
Tel: +62-274-413668, e-mail: wwilopo@gadjahmada.edu

[2] Department of Earth Resources Engineering, Kyushu University, Fukuoka, Japan,
Tel: +81-92-802-3337, e-mail: hirajima@mine.kyushu-u.ac.jp

Abstract

Sorption and precipitation of manganese in groundwater remediation using compost and zero-valent iron (ZVI) were investigated by batch and column experiments. In batch tests, compost is more effective than ZVI to immobilize manganese, with the maximum removal of 238.09 mmol Mn. kg^{-1} of compost according to Langmuir equation. High efficiency of Mn removal onto compost is probably not only by physical sorption but also by surface complexation with carboxylic groups in the compost. This result was confirmed with FTIR data that shown new peaks at 675 cm^{-1} after contacted with manganese solution. Manganese was also immobilized through sorption onto ZVI due to high surface area, and partly by precipitation as manganese oxide because of intense alkalization. In column materials, after introducing manganese solution for 36 pore volumes (pv), manganese was predominantly immobilized in upper part of the column. It is considered that compost was degraded and the surface of ZVI granules was already uniformed and corrosion products are the most accumulated on ZVI granules near the inlet because ZVI has been contacted with high concentrations of manganese for the longest time in the most bottom parts. This was also supported by XRF data from ZVI grains that manganese was the largest in the most bottom segment. The results of geochemical calculations along with the SEM image suggest that partly of manganese were also precipitated with carbonates. The result demonstrates that combination of compost and ZVI is more effective to remove manganese than using single material due to the different mechanism of removal from each material.

Introduction

Manganese is an essential element for humans and other animals, however intake of excess Mn leads to nervous system problems, lung embolism and bronchitis [1]. In order to minimize the effect of manganese, WHO regulated the concentration of Mn in drinking water and industrial drainage less than 0.4 mg dm^{-3} and 10 mg dm^{-3}, respectively [2]. The most important oxidative states for the environment and biology are Mn(II), Mn(IV) and Mn(VII). Manganese is naturally occurring in many surface water and groundwater sources, particularly in anaerobic or low oxidation conditions, and this is the most important source for drinking-water. The source of Mn is mainly from rock such as andesite, diorite, basalt, shale and sandstone [3]. Some organic materials also have been reported to release Mn into the environment [4].

Manganese is notoriously difficult to remove using both active and passive treatment because of the high activation energy required for Mn oxide precipitation [5]. The Mn oxide does not readily occur without supporting highly oxidizing and/or high pH [6]. Abiotic Mn-removal using limestone-filled columns or a reactor filled with dolomite raise the pH for Mn oxidation and subsequent precipitation [7][8]. Although manganese readily precipitates as Mn(IV), little oxidation of Mn(II) occurs in solutions below pH 8, as the kinetics for manganese oxidation are slow relative to that of Fe(II) [9]. In addition, biological oxidation of Mn(II) does not proceed rapidly in the presence of Fe(II), and thus it is not removed significantly in aerobic wetlands where the concentration of ferrous iron exceeds 1 mg/l [10].

Manganese does not readily form an insoluble sulfide phase and thus it is not removed to a great extent by sulfate-reducing bioreactors, though it may precipitate in these systems as rhodocrosite ($MnCO_3$) [11]. As manganese is generally not efficiently removed by current passive technologies applied to remediate manganese contaminated groundwater, alternative approaches are needed.

Permeable reactive barriers (PRBs) is one of the passive and *in-situ* groundwater treatment techniques for organic and inorganic contaminants, including chlorinated solvents, petroleum hydrocarbons, selected pesticides, chromium and other heavy metals, nitrate, phosphate and sulfate-rich mine drainage [12]. When the contaminated plume goes through the barrier, the contaminant species react with barrier materials to reduce the concentration based on sorption, precipitation and decomposition. Chemical and microbiological reactions can be involved in the process of PRBs. It has several advantages to enable the usage of ground surfaces for the other objectives and to save the operation and maintenance cost without facility and electricity [13]. These advantages are more desirable and acceptable as monitoring natural attenuation (MNA) in modern environmental technologies than conventional methods. One direction of development in PRBs researches is to find the cost effective reactive materials.

The objective of this research is to investigate of the possibility of mangese removal in the PRB using zero valent iron (ZVI) and compost as a passive treatment for mine tailing filtrates from Sumbawa Island, Indonesia.

Experimental

The reactive materials consisted of ZVI and compost. The ZVI was provided by Connelly-GPM™, Chicago, Illinois, USA. Zero valent iron is elemental metallic iron, reduces waterborne inorganic ions, releasing soluble Fe(II) in their place, which oxidizes further into Fe(III).Compost was provided by local company. Compost is cheaper and easy to find than ZVI, however it easy to degrade because of an organic material. Table 1 shows the physical properties of each material. The elemental compositions of ZVI and compost were summarized in Table 2.

Table 1. Physical Properties of Each Material

Materials	Density (g cm^{-3})	Diameter (mm)	Surface Area (m^2 g^{-1})
ZVI	2.24 - 2.56	2.38-2.97	2.4
Compost	0.38	0.1 – 5	-

Note : "-" no data

Table 2. Chemical Composition of Each Material

Materials	Components (% w/w)							
ZVI	Fe	C	Mn	Ni	P	Si	Cu	Mo
	89.82	2.85	0.6	0.05-0.21	0.132	1.85	0.15-0.20	0.15
Compost	H_2O	C	N	S	Others			
	54.48	41.34	1.91	0.05	2.22			

Batch Tests

Several batch tests were performed to determine the best materials to remove Mn(II) from low cost materials. One gram of sterilized ZVI and 2 grams of compost were used to find the sorption isotherm of Mn onto each material using 0.25 dm^{-3} solutions containing different concentrations of Mn(II) with initial pH 6.25. All solutions of Mn(II) were prepared using $MnSO_4.5H_2O$ special grade from WAKO. Nitrogen gas was purged for 20 min to remove dissolved oxygen in the solutions. All solutions were shaken at 100 rpm and $25^{o}C$ until sorption equilibrium was attained. The pH was measured using TOA WM-22EP GST-2729C electrodes. Manganese concentration was determined by VISTA-MPX ICP-OES (Seiko Inst., Japan).

Column Tests

Simulated groundwater for column tests was prepared using chemical reagents, based on the composition of Mn-contaminated groundwater found at Sumbawa, Indonesia [14]. The groundwater has been impacted by the geological condition of the area resulted in the high concentration of manganese. The chemical composition of groundwater as follow: K^+ (26.34 mg/L), Ca^{2+} (27.43 mg/L), Mg^{2+}(14.36 mg/L), Na^+ (8.27 mg/L), CO_3^{2-} (76.53 mg/L), Cl^-(127.6 mg/L), SO_4^{2-} (104.80 mg/L), NO_3^- (0.61 mg/L), Mn^{2+} (15.1 mg/L) and pH 6.2. The manganese concentrations were spiked to be mostly 4 times of actual groundwater to evaluate the treatability within the restricted periods. The simulated groundwater was prepared as follows (in gram per 1 liter of deionized water): $MnSO_4.5H_2O$ (0.263), $CaCO_3$ (0.069), $MgCO_3$ (0.065), KNO_3 (0.001). The pH was adjusted to 6.25 ± 0.25 with 1 mol dm^{-3} HCl and 1 mol dm^{-3} NaOH. The solution was purged with nitrogen gas for 2 h to minimize the content of dissolved oxygen and kept under anaerobic conditions prior to use.

The PRB column tests were performed using one acrylic cylindrical column with 40 cm in height, 7.5 cm in inner diameter, 13 side ports along the vertical direction, and approximately 1767.86 cm^3 in internal volume. The bottom layer (1.5 cm) and top layer (1.5 cm) of the column packing consisted of 100% glass beads (0.6-0.8 mm in diameter) as non reactive material. The middle reactive layer was composed of 5(v/v)% ZVI, 23(v/v)% compost, 22(v/v)% woodchips, 30(v/v)% glass beads, and 20(v/v)% gravels. The same ZVI and compost using in the batch experiments are used as the reactive materials here. In order to maintain the permeability of the column, glass beads (average ø 0.5 mm) and gravels (average ø 12 mm) were added as unreactive materials. All materials were sterilized by autoclaving at 121 ^{o}C for 20 minutes. Then, all materials were mixed homogeneously, filled uniformly in the columns, and nitrogen gas was purged for 12 h to generate anaerobic conditions according to the previous PRB works.[15] The porosities were gravimetrically determined to be 37.4%. The flow rate of influent was initially set at 0.21 cm h^{-1} from the bottom to the top by peristaltic pumps (EYELA 10413787, Rikakikai Co. Ltd., Japan), resulting in 2.78 days of residence time, and monitored regularly. All experiments were conducted in an anaerobic glove box (COY, Michigan, USA) purged with a gas mixture containing of 95% N_2 and 5% H_2.

Effluent solutions were regularly collected twice a week, while 36 times of pore volume of influent solutions travels. Pore volume (pv) is defined as the required time to travel for the influent from the bottom to the top of the column and used as a time unit. At pv 36 the side-port samples were taken from each column. Temperature, pH, redox potential, and alkalinity were measured immediately after sample collection. Temperature and pH were measured using TOA WM-22EP GST-2729C electrodes, the redox potential was determined using TOA RM-20P PST-2739C electrodes and converted to *Eh* vs NHE. Alkalinity was determined using a Hach[TM] digital titrator (Titration Method 2320B; American Public Health Association (APHA), 1992). The determination of Mn concentrations is the same with in the batch tests. Major anions and cations were determined using a Dionex DX-120 ion chromatograph. Other heavy metal concentrations were determined by an inductively coupled plasma optical emission spectrometer VISTA-MPX ICP-OES (Seiko Inst., Japan). Saturation index (SI) for representative minerals was calculated using a geochemical calculation code of MINTEQA2 [16]. After taking side ports samples at pv 36, the column materials were also taken by decomposing the columns under anaerobic condition. Residual materials in a reactive zone were divided into 10 fractions along the water traveling direction as follows: 1.5 – 5.2 cm, 5.2-8.9 cm, 8.9-12.6 cm, 12.6-16.3 cm, 16.3 – 20 cm, 20-23.7 cm, 23.7-27.4 cm, 27.4-31.1 cm, 31.1-34.5 cm and 34.8-38.5 cm from the bottom of the column. The residual ZVI granules were separated using a magnet covered with a plastic bag from PRB materials in an anaerobic glove box, to provide for X-ray diffraction (XRD; RINT-2100, Rigaku), scanning electron microscopy (SEM, VE-9800, Keyence Co.) and energy dispersed X-ray analysis (EDX, EDAX Genesis, EDAX Japan Co., Ltd.).

Results and Discussion

Batch Tests

The raw data for sorption curves of Mn onto compost and ZVI at 25°C were presented in Figure 1. The equilibrium pHs of the solutions from compost are 6.51-5.04, almost of them are lower than the initial pH. However, the equilibrium pHs of ZVI are 10.27 - 6.55, higher than the initial pH. Freundlich isotherm model was fitted to the equilibrium data of sorption isotherm of manganese onto compost and ZVI following the equation:

$$\log Q = \log K_f + n \log C_e \qquad (1)$$

Where Q is the sorbed manganese per unit amount of sorbents (mmol kg^{-1}) at the equilibrium, C_e is equilibrium concentration of manganese (mmol dm^{-3}), and K_f and n are constants represent the adsorption capacity and adsorption intensity of the adsorbent, respectively [17]. The results of the fitting model with the data are shown in Figure 2 and Table 3. It shows that compost is more effective sorbent for Mn removal with adsorption capacity 268.66 mmol kg^{-1}.

In addition, Langmuir isotherm model was also fitted to the sorption isotherm data of Mn onto ZVI, GBFS and compost following this equation:

$$Q = \frac{q_{\max} C_e}{\left(C_e + K_d\right)} \qquad (2)$$

Where Q_{max} is the maximum of sorbed manganese per unit amount of sorbents (mmol kg^{-1}), K_d is the dissociation coefficient of the solute-adsorbent complex which represents the affinity between the solute and the adsorbent. The results of fitting model with the data

are summarized in Figure 2 and Table 4. Compost shows the best sorbent for Mn removal with the maximum removal 238.09 mmol Mn. kg^{-1} of compost.
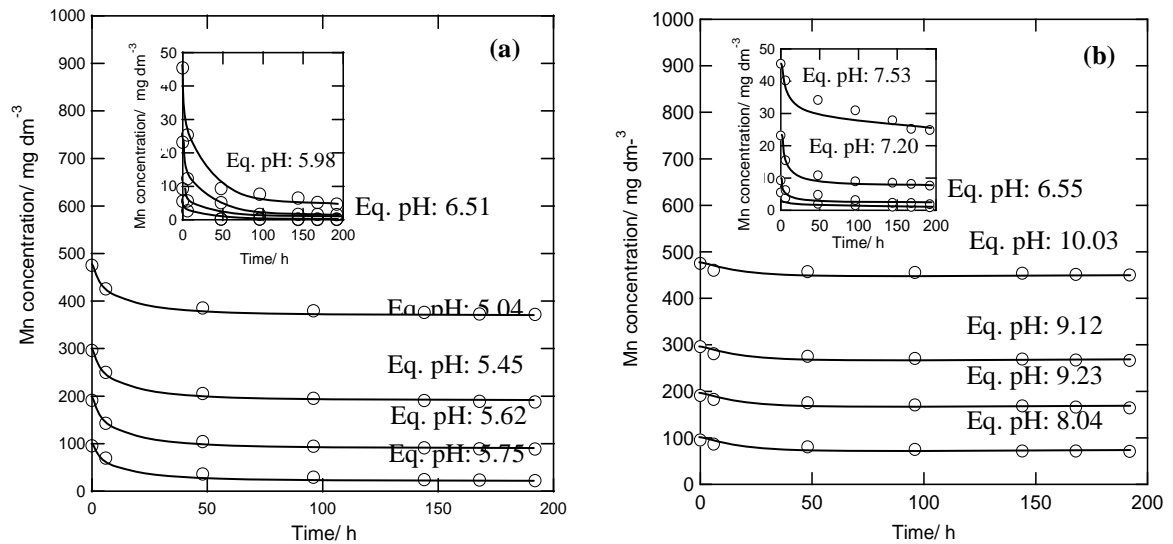

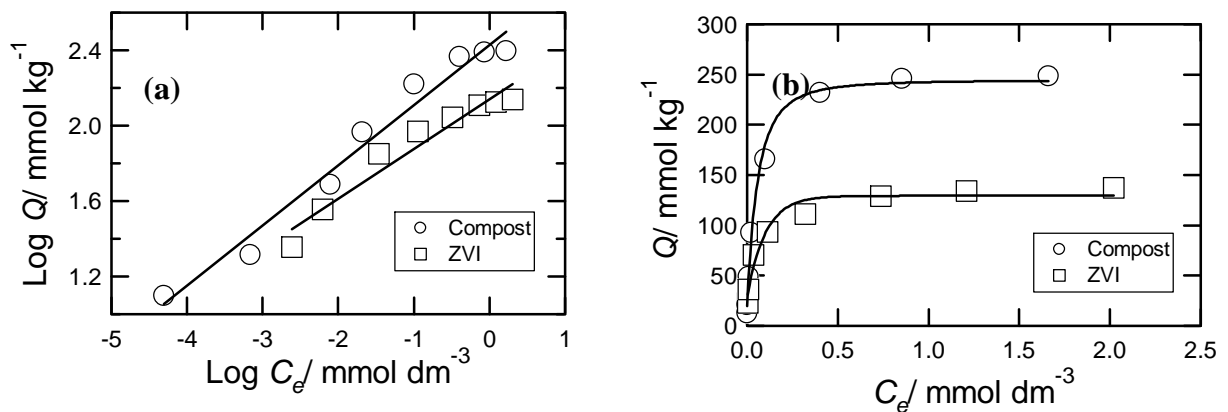Figure 1. Sorption of Mn^{2+} onto (a) compost and (b) ZVI at initial pH 6.25 and 25°C

Figure 2. (a) Linearized Freundlich plots for sorption of manganese onto compost and ZVI.
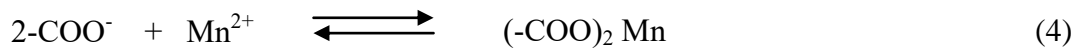(b) Plots for sorption of manganese onto compost and ZVI showing Langmuir isotherm fits to the data

Table 3. Summary of Freundlich Constants for Sorption of Mn onto ZVI and Compost

Sorbent	K_f	n	R^2
ZVI	137.75	0.26	0.94
Compost	268.66	0.32	0.97

Table 4. Summary of Langmuir Constants for Sorption of Mn onto ZVI and Compost

Sorbent	Q_{max} (mmol kg^{-1})	K_d	R^2
ZVI	129.87	38.50	0.95
Compost	238.09	42.00	0.99

High Mn removal in the compost was mainly by physical sorption and also complexation, due to decrease of equilibrium pHs from the initial pH. This suggests that Mn binding to the biomass is associated with the release of H$^+$ ions into the solution, following this reaction:

$$\text{-COOH} \quad \rightleftarrows \quad \text{COO}^- + \text{H}^+ \qquad (3)$$

$$2\text{-COO}^- + \text{Mn}^{2+} \quad \rightleftarrows \quad \text{(-COO)}_2\,\text{Mn} \qquad (4)$$

This clearly indicates that the mechanism of Mn binding involves complexation mechanisms, possibly, the Mn ions react with hydroxyl or carboxylic groups of the compost releasing H$^+$ ions into the solution. Figure 3 shows FTIR of compost before and after reactions with Mn solution. It shows that after contact with Mn solution, peak was observed at around 675 cm^{-1}, which is caused by stretching vibration of Mn-O bonds [18]. In the ZVI, manganese mainly will be immobilized by physical sorption as a result of high surface area. In addition, some of manganese also will be precipitated as manganese oxide due to high pH (pH >8.5).
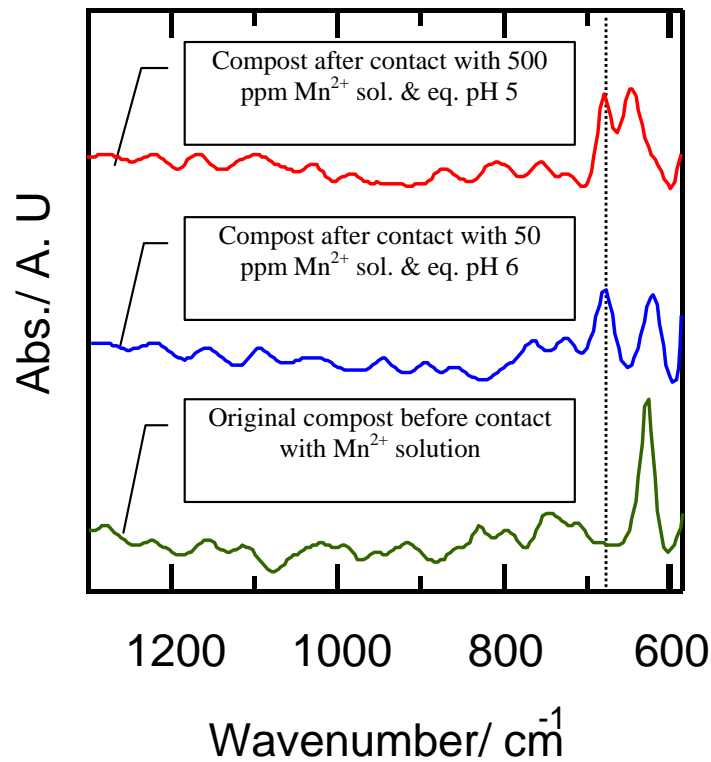

Figure 3. FTIR spectra of the compost before and after contact with Mn solution (50 and 500 mg/L)

Column Tests

Changes of pH, Eh, alkalinity, and temperature during the column experiments are presented in Figure 4. Initially, pH increased from 6.25 in the influent to around 7 in the effluent and then decreased after pv 34. It is known the reactions of ZVI with H_2O and H^+ produce OH- (Equation 5) and H2 (Equation 6) [15]. The pH increased until pv 34 according to the reactions, but became stable after pv 34, probably due to changes of the surface on ZVI to less active.

$$2Fe^0 + 2H_2O + O_2 \rightleftharpoons 2Fe^{2+} + 4OH^- \qquad (5)$$
$$Fe^0 + 2H^+ \rightleftharpoons Fe^{2+} + H_2 \qquad (6)$$
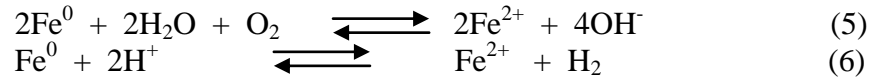
Eh decreased in the column throughout the experiments, indication that the above reduction occurred. Alkalinity in the effluent was higher but after pv 25, it suddenly dropped to similar values to those of the influent. Temperature varied from 26^oC to 20^oC, depending on season but it did not change during transportation in the columns.

Time courses of major ions in the columns are shown in Figure 5. Sodium, magnesium, and potassium concentration initially showed increase in the effluent, then after pv 3, they increased to reach a balance with those in the influent until the end of the experiment (Figure 5(a),(b),(c)). However, calcium concentrations in the effluent are higher than in the influent until the end of experiment probably due to leaching from organic materials and gravels. Figures 5(e) and 5(f) shows the chloride and sulfate concentration were relatively conservative during the experiment.
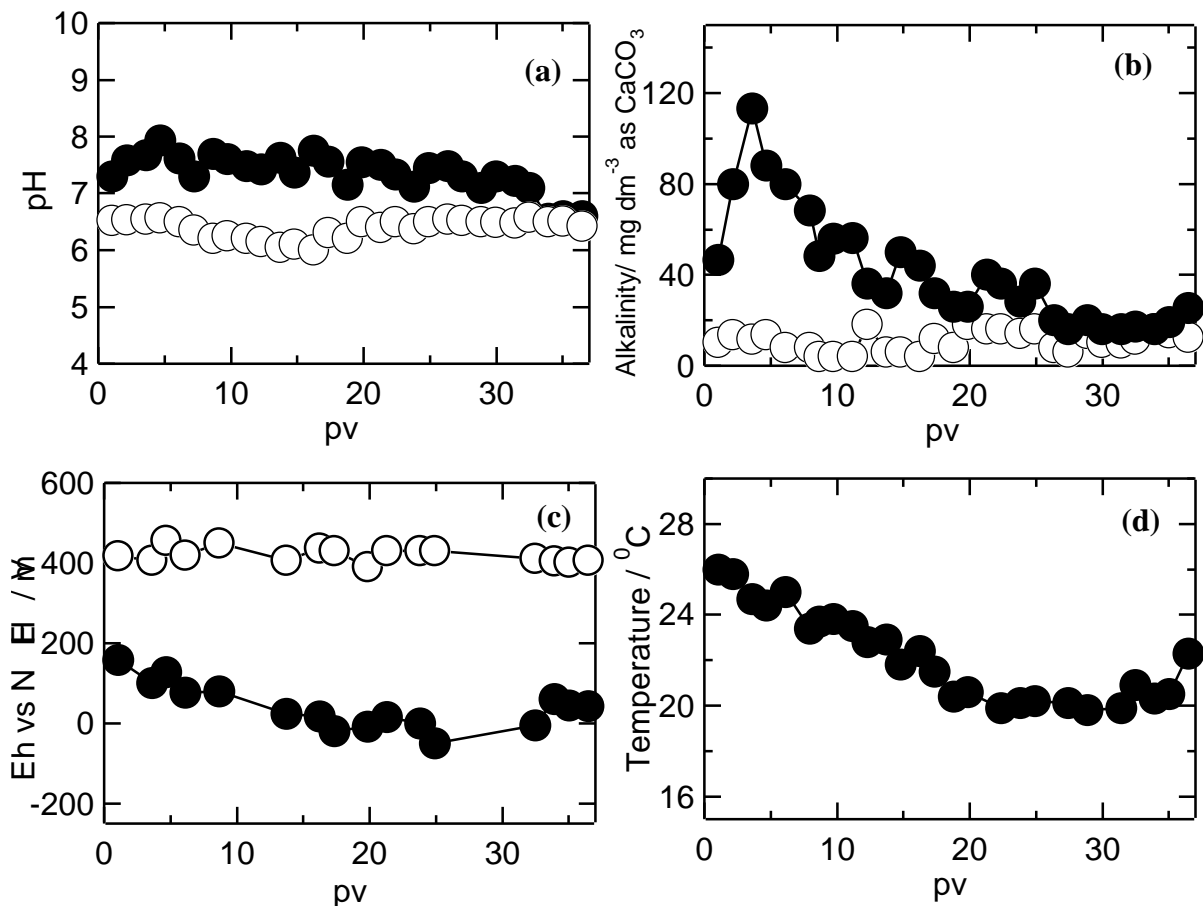

Figure 4. Changes of (a) pH, (b) Eh, (c) alkalinity, and (d) temperature in the columns with pv. The open and solid symbols indicate influent and effluent, respectively.
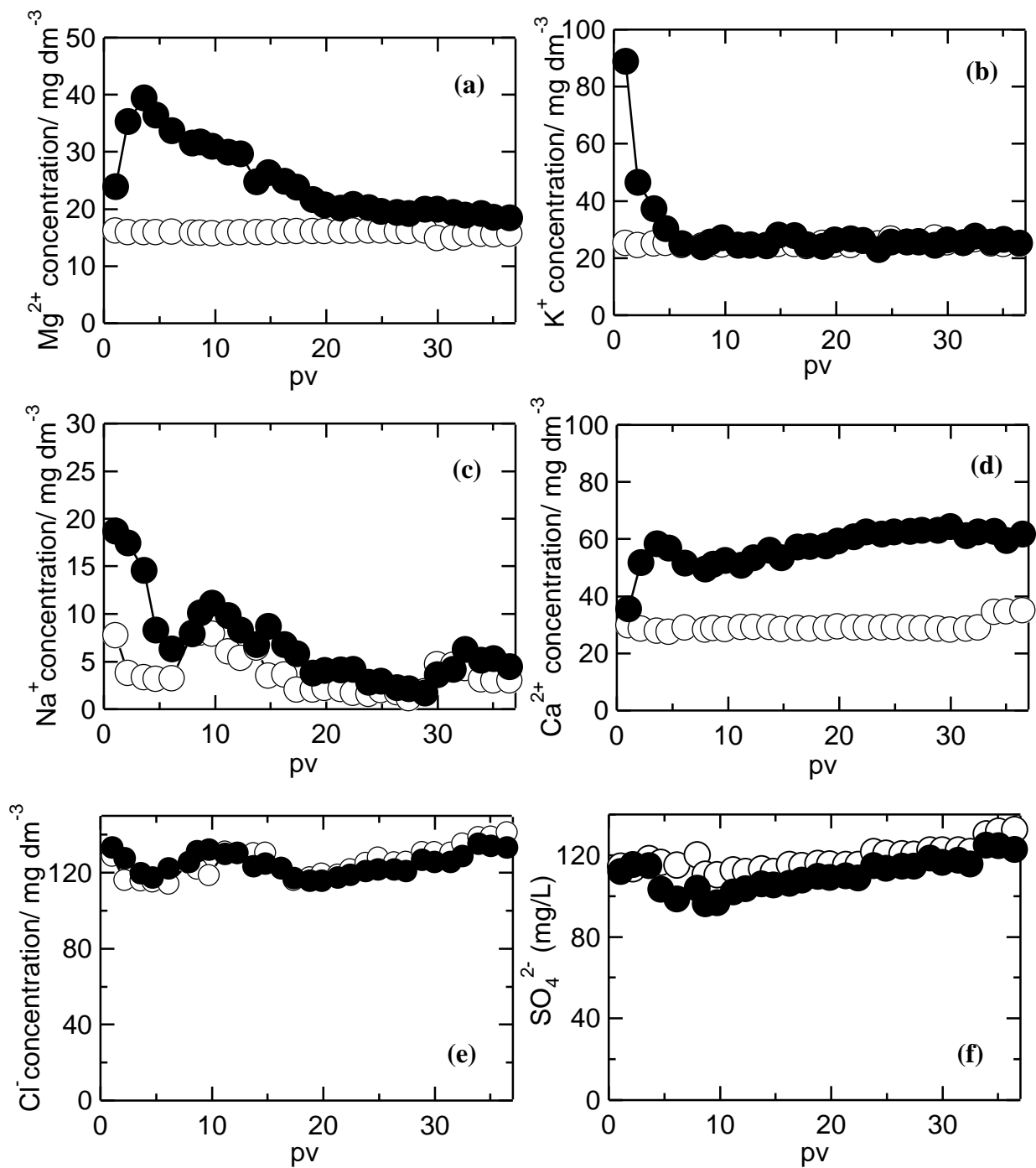
Figure 5. Changes of major ions, (a) Ca^{2+}, (b) K^+, (c) Mg^{2+}, (d) Na^+, (e) Cl^- and (f) SO_4^{2-} in the columns with pv. The open and solid symbols indicate influent and effluent, respectively

Changes of Mn^{2+} concentrations in the column are illustrated in Figure 6(a). Manganese has been removed in the column under the MCL until pv 30. With the Q_{max} value of compost and ZVI are 238.09 mmol kg^{-1} and 129.87 mmol kg^{-1}, respectively. Therfore, 2016.62 grams of Mn should be immobilized on the loaded compost and ZVI in the column. However, the total of Mn accumulated in the column was calculated to be 1701.08 mg. It suggests that column has still more capacities of sorbents for sorption of Mn^{2+}. The presence of other major cations are competitive species to Mn^{2+} sorption onto compost, therefore, Mn removal was less effective in the column than in the batch tests. Manganese in the column showed rapid decrease in lower than 8 cm column height (Figure 7(a)) as a sorption mechanism, than slowly decrease over 8 cm column height probably from precipitates as manganese carbonate due to inlet of the contaminated groundwater from the bottom. This result is also consistent with the XRF data from remaining ZVI grain after decomposing of column materials in Figure 7(b) that showed high concentration of Mn in the bottom part of the column. High concentrations of iron were initially in the effluent until pv 3 probably due to leaching of ZVI as shown in Figure 6(b).
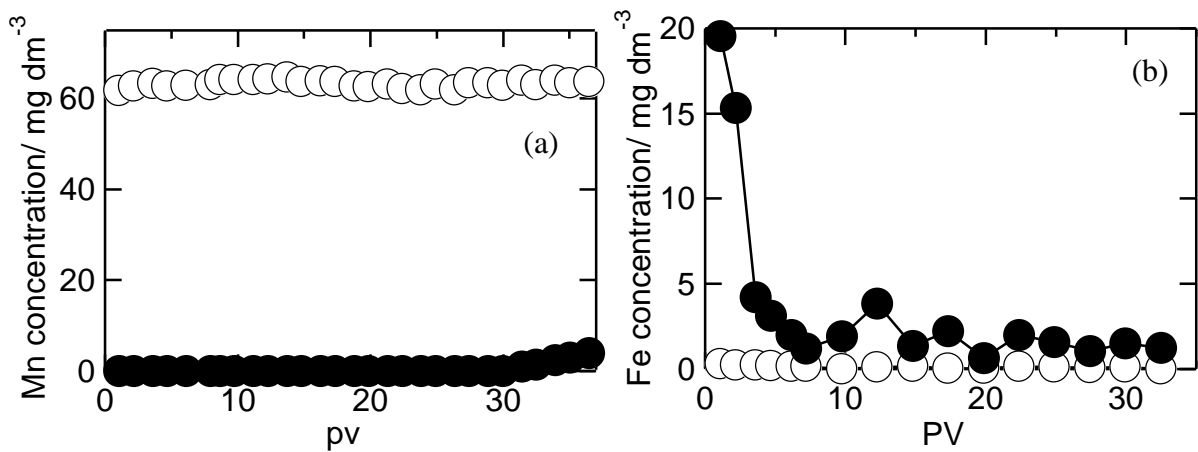

Figure 6. Changes of (a) Mn and (b) Fe concentrations in the column with pv. The open and solid symbols indicate influent and effluent, respectively
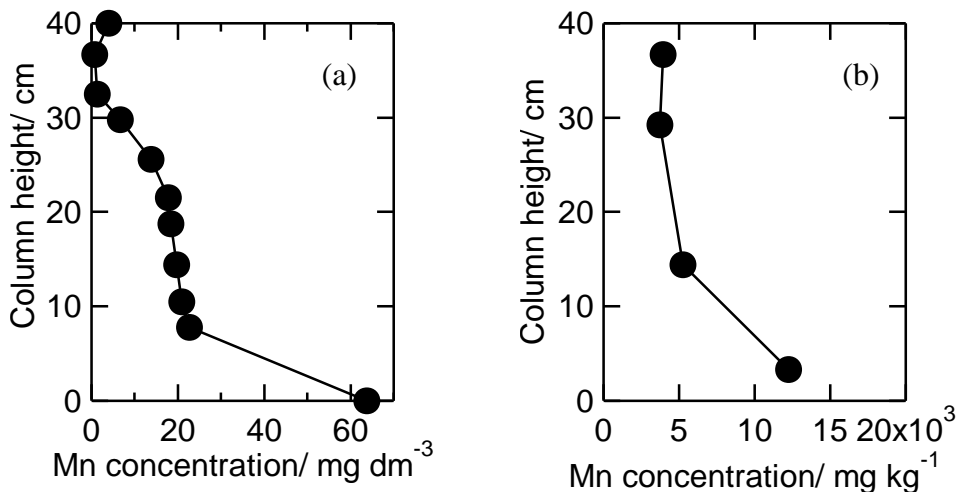

Figure 7. (a) Vertical profile of for Mn in the column at pv 36 and (b) Vertical Profile of Mn contents in residual ZVI grains at PV 36

Some of Mn were probably also precipitated as rhodocrocite ($MnCO_3$) due to high pH and high alkalinity until pv 19. This interpretation was supported by positive SIs for $MnCO_3$ in the results of MINTEQA2 in Figure 8(a) and SEM image data in Figure 9. The solubility product of rhodocrocite is smaller than calcium carbonates, which is likely to precipitate in Figure8(a) [19]. However, after pv 25 the precipitation of $MnCO_3$ became unlikely with decrease in alkalinity. The mechanism of Mn removal largely, depends on sorption to compost and ZVI because of less alkalinity.
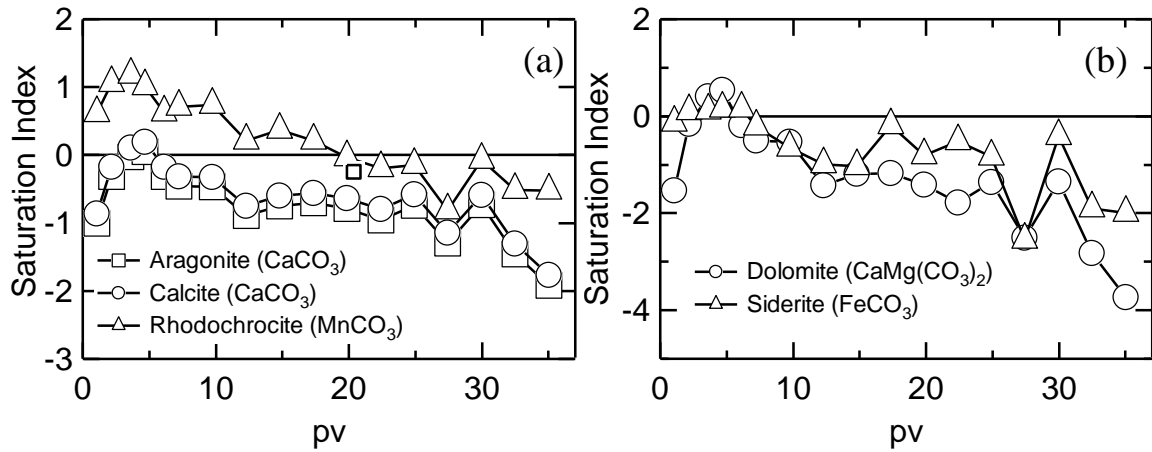

Figure 8. Saturation indexes of some minerals in the column. (a) $CaCO_3$ and $MnCO_3$; (b) other carbonates
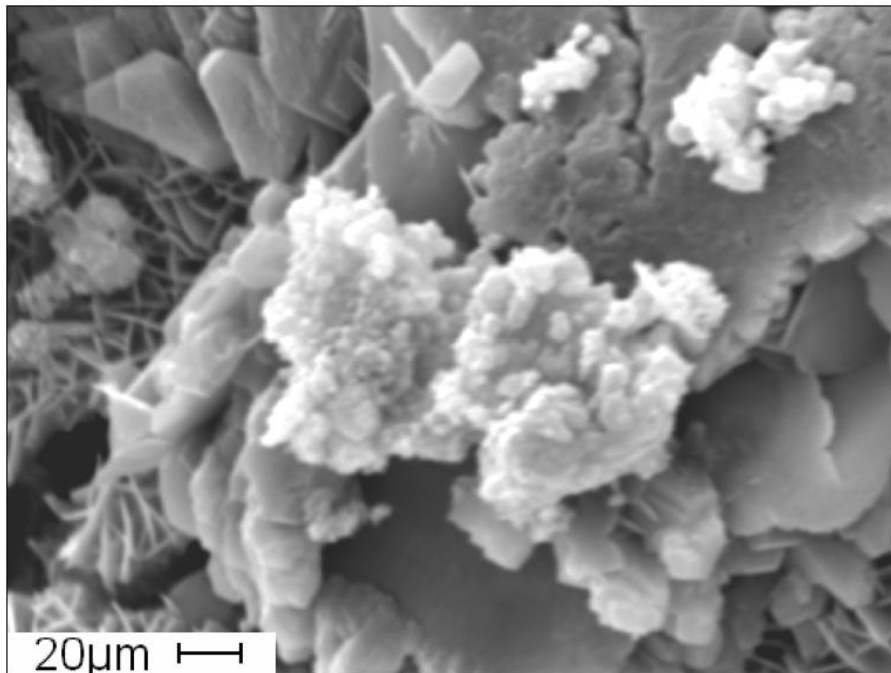

Figure 9. SEM image of ZVI grain from the fraction of 1.5 - 5.2 cm from the bottom of column at pv 36 showed a precipitated mineral is likely rhodocrocite (MnCO3)

Conclusions

The removal of Mn was investigated using batch and PRB column experiments. The result from batch experiment showed that compost and ZVI is a good sorbent for manganese removal in water. The mechanism of Mn removal was mainly explained by sorption onto compost and ZVI, and partly precipitation as rhodocrocite. Even though compost is more effective to remove manganese than ZVI, however a combination both compost and ZVI can increase removal capacity. ZVI raises pH of solution that would be facilitating precipitation of manganese. The presence of other major cations are competitive species to Mn^{2+} sorption onto compost and ZVI in the column experiment, therefore, manganese removal was less effective in the column than in the batch tests.

Acknowledgements

References

[1] United States Environmental Protection Agency, *EPA's 2007 Report on the Environment: Science Report (Sab Review Draft)*, EPA/600/R-07/045, Office of Research and Development, Washington, D.C., United States, 2007.

[2] World Health Organization (2004). *Guidelines for Drinking-Water Quality,* 3rd ed., Vol. 1 Recommendations, Genewa, Switzerland.

[3] R.J. Gilkes, and R.M. McKenzie, "Geochemistry and mineralogy of manganese in soils," In *Manganese in Soils and Plants*, R.D. Graham, R.J. Hannam, and N.C. Uren, eds.: Kluwer Academic Publishers, Dordrecht, The Netherlands, pp. 23–35, 1988.

[4] K.V. Heal, "Manganese and land-use in upland catchments in Scotland," *The Science of the Total Environment*, Vol. 265, pp. 169-179, 2001.

[5] D.A. Crerar, and H.L. Barnes, "Deposition of deep-sea manganese nodule," *Geochimica et Cosmochimica Acta*, Vol. 38, Issue 2, pp. 279-300, 1974.

[6] F.J. Sikora, L.L. Behrends, G.A. Brodie, and H.N. Taylor, "Design criteria and required chemistry for removing manganese in acid mine drainage using subsurface flow wetlands," *Water Environment Research*, Vol. 72, pp. 536-544. 2000.

[7] F.C. Thornton, "Manganese removal from waters using limestone filled tanks," *Ecological Engineering*, Vol. 4, No. 1, pp. 11-18, 1995.

[8] K.L. Johnson, "The importance of aeration in passive treatment schemes for manganese removal," *Land Contamination & Reclamation*, Vol. 11, pp. 205–212, 2003.

[9] J.J. Morgan, and W. Stumm, "Colloid-chemical properties of manganese dioxide," *Journal of Colloid and Interface Science*, Vol. 19, pp. 347–359, 1964.

[10] B. Nairn, and R.S. Hedin, "Contaminant removal capabilities of wetlands constructed to treat coal mine drainage" In *Constructed Wetlands for Water Quality Improvement*, G.A. Moshiri, ed.: Lewis Publishers, Boca Raton, Florida, United States, pp. 187–195, 1993.

[11] K.B. Hallberg, and D.B. Johnson, "Biological manganese removal from acid mine drainage in constructed wetlands and prototype," *Science of the Total Environment*, Vol. 338, pp. 115-124, 2005.

[12] R.M. Powell, R.W. Puls, D.W. Blowes, J.L. Vogan, R.W. Gillham, P.D. Powell, D. Schultz, T. Sivavec, and R. Landis, *Permeable Reactive Barrier Technologies for Contaminant Remediation*, Report No. EPA/ 600/R-98/125, Enviromental Protection Agency, 1998.

[13] R.W. Puls, C.J. Paul, and R.M. Powell, "The application of in situ permeable reactive (zero-valent iron) barrier technology for the remediation of chromate-contaminated groundwater: A field test," *Applied Geochemistry*, Vol 14, No. 8, pp. 989-1000, 1999.

[14] PT Newmont Nusa Tenggara, *Environmental Management and Monitoring Report; 4th quarter October –December 2003; Annual Report 2003; and Annual Plan 2004*, 2004.

[15] K. Sasaki, D.W. Blowes, and C.J. Ptacek, "Spectroscopic study of precipitates formed during removal of selenium from mine drainage spiked with selenate using permeable reactive materials," *Geochemical Journal*, Vol 42, pp. 283-294, 2008.

[16] United States Environmental Protection Agency, *MINTEQA2*, 2011. Retrieved from http://ww.epa.gov/ceampubl/mmedia/minteq/indeq.htm

[17] A.A. Lewinsky, *Hazardous Materials and Wastewater*, Nova Publishers Inc., New York, 2007.

[18] W. Tong, G. Xia, Z. Tian, J. Liu, J. Cai, S.L. Suib, and J.C. Hanson, "Hydrothermal synthesis and characterization of sodium manganese oxo-phosphate $Na_2Mn_2O(PO_4)_2 \cdot H_2O$," *Chemistry of Materials*, Vol. 14., pp. 615 – 620, 2002.

[19] D.L. Jensen, J.K. Boddum, J.C. Tjell, and T.H. Christensen, "The solubility of rhodochrosite ($MnCO_3$) and siderite ($FeCO_3$) in anaerobic aquatic environments," *Applied Geochemistry*, Vol. 17, pp. 503-511, 2002.